Suppression of Stimulated Brillouin Scattering in Single-Frequency Fiber Raman Amplifier Through Pump Modulation

Achar Vasant Harish and Johan Nilsson, *Fellow, OSA*

***Abstract*—We propose and implement the use of an intensity-modulated pump, counter-directional to a forward-propagating signal for suppressing unwanted stimulated Brillouin scattering (SBS) of spectrally narrow signals in optical fiber Raman amplifiers. The modulated Raman pump cross-phase modulates and thus spectrally broadens the parasitic Brillouin Stokes wave traveling in the same (backward) direction. The parasitic SBS then decreases when the broadening exceeds the Brillouin gain bandwidth. By contrast, the modulated pump does not induce any significant cross-phase modulation on the signal, which therefore can remain spectrally narrow. We study the effect of the pump modulation frequency and modulation format and experimentally obtain nearly 5 dB of SBS threshold enhancement and over 50% pump-to-signal conversion efficiency.**

***Index Terms*—Amplifiers, Brillouin scattering, optical fiber amplifiers, Raman scattering.**

I. Introduction

STIMULATED Brillouin scattering (SBS) [1], [2] is a major obstacle for power scaling of fiber amplifiers with signal linewidths narrower than the SBS bandwidth, typically in the range 10-100 MHz in silica fibers. This includes so-called single-frequency signals, e.g., as generated by lasers operating on a single longitudinal mode. Such signal light, acting as the Brillouin pump, generates an acoustic wave through electrostriction and is then readily Brillouin-scattered into a counter-propagating Brillouin Stokes wave when the associated Brillouin gain becomes sufficiently high. The Brillouin Stokes wave leads to signal-wave depletion, which is generally unwanted. In fiber Raman amplifiers (FRAs), the problem of unwanted SBS is exacerbated by the relative weakness of stimulated Raman scattering (SRS) and the resulting need for large intensity-length product often achieved through the use of long fibers [3]. Both SBS and SRS are third-order nonlinear effects which scale in the same way with fiber length and effective area. However, for single-frequency signals, SBS is two to three orders of magnitude stronger than SRS in silica fibers [4], [5]. Therefore, a single-frequency signal will induce unacceptable levels of SBS already at signal powers that are too weak to induce significant levels of SRS and thus power transfer from the Raman pump. This hinders efficient operation and power-scaling of FRAs for single-frequency signals.

Several methods have been proposed to suppress unwanted SBS in optical fibers, including FRAs. Temperature [6] and strain variations [7], including temperature variations induced by the amplification itself [2], [8], have been used to shift and broaden the Brillouin gain spectrum, and thus reduce the peak gain. Some work has also focused on fabricating specially-designed fibers, including fibers with acoustically tailored properties [9]–[12] and longitudinally varying characteristics [13], [14]. However, these approaches are hampered by the need for special fibers or fiber arrangements that are not fully proven, and are not uniformly adopted.

Instead, signal linewidth broadening [15], [16] may be the most common approach for SBS suppression. Often, an electro-optic phase modulator is used to broaden the spectrum. Alternatively, spectral broadening can be realized directly inside the fiber through cross-phase modulation (XPM) [17]–[19]. In one of the earliest studies, XPM induced by co-propagating intensity-modulated WDM signals were used to broaden the linewidth of each signal and thus suppress SBS in an optical communication link [20]. This technique can also be considered for FRAs if XPM by an intensity-modulated Raman pump broadens the linewidth of an amplified signal wave which would otherwise induce SBS [21]. The pump and signal must propagate in the same (forward) direction for efficient spectral broadening in this scheme, since XPM is negligible for counter-propagating waves insofar as the pump modulation is sufficiently fast to be averaged out within the fiber transit time. However, one drawback with this and any other approach that spectrally broadens the signal is that it cannot be used in applications that require linewidths narrower than the Brillouin bandwidth, including single-frequency signals. Also, because the Raman gain buildup is practically instantaneous in a FRA, a co-propagating intensity-modulated pump would intensity-modulate the signal, which is often undesired.

In this paper we propose a novel method for suppressing SBS in a FRA, where we modulate and thus spectrally broaden the

Manuscript received January 17, 2019; revised March 26, 2019; accepted April 8, 2019. Date of publication April 30, 2019; date of current version June 5, 2019. This work was supported in part by Engineering and Physical Sciences Research Council (EP/H02607X/1) and in part by the Air Force Office of Scientific Research under Grant FA2386-16-1-0005. *(Corresponding author: Achar Vasant Harish.)*

The authors are with the Optoelectronics Research Centre, University of Southampton, Southampton SO17 1BJ, U.K. (e-mail: harish5089@gmail.com; jn@orc.soton.uk).

Color versions of one or more of the figures in this paper are available online at http://ieeexplore.ieee.org.

Digital Object Identifier 10.1109/JLT.2019.2914081

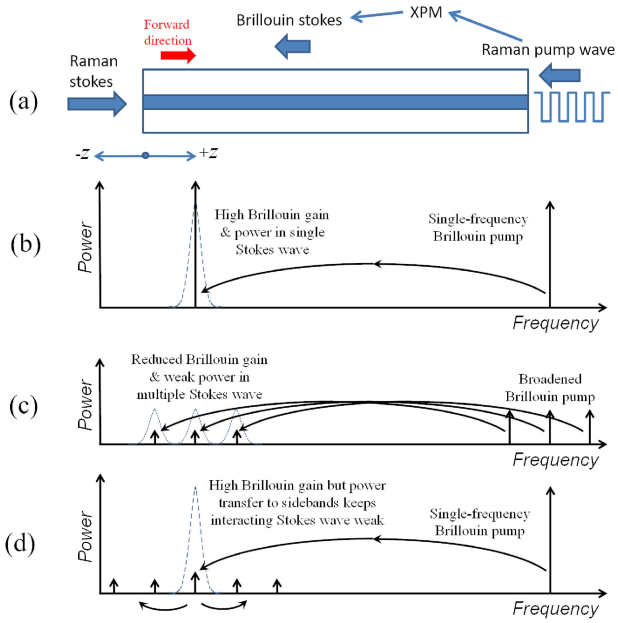

Fig. 1. (a) Schematic diagram of an optical fiber showing the signal (i.e., the Raman Stokes) and the intensity modulated Raman pump wave inducing XPM on the Brillouin Stokes, (b) schematic spectrum of the SBS process showing power transfer from a single-frequency Brillouin pump to a single Stokes line, (c) schematic spectrum of the SBS process showing power transfer from a spectrally broadened Brillouin pump to multiple Stokes lines with reduced Brillouin gain, and (d) schematic spectrum showing the novel approach with a single-frequency Brillouin pump and multiple Stokes lines generated by cross-phase modulation with reduced SBS power transfer due to a reduced interaction with the Stokes wave.

Stokes wave. Advantageously, it does not rely on any signal linewidth broadening. Since the Brillouin Stokes wave is generated inside the fiber without any seeding and therefore cannot be modulated externally, we instead modulate it inside the fiber, through XPM from an intensity-modulated Raman pump co-propagating with the Brillouin Stokes wave in the backward direction. This reduces the SBS, even when the cross-intensity modulation and the XPM-induced spectral broadening of the forward-propagating Raman-amplified signal are negligible. Similar idea was previously exploited in [22] to use noisy Raman pump to suppress Rayleigh backscattering. This noisy nature of the pump could also lead to increase in Raman ASE under certain circumstances, as discussed in [23].

Figure 1 illustrates our scheme for SBS suppression through XPM-induced Stokes broadening, which we demonstrate through both numerical simulations and experiments. We first describe a finite-difference model of a FRA that is limited by SBS, and present results of simulations. We then describe the experimental setup and results using a fiber in the normal dispersion regime. We experimentally investigate the pump modulation formats for best SBS suppression and pump with pulses of varying duty cycle and repetition frequency.

II. Simulations

To start, we describe our method in greater detail and present results of simulations. These results are examples rather than a full investigation of the parameter space. In particular, it was not possible to use the experimental parameters in the simulations. SBS and other nonlinearities of arbitrarily polarized waves are complicated and hence we model waves linearly polarized in the same direction. This assumption leads to maximum nonlinear interaction in the optical fiber. There are four waves propagating inside the FRA, which can be modeled by the following equations [24], [25].

$$\frac{\partial E_P}{\partial z} - \frac{n}{c}\frac{\partial E_P}{\partial t} = -\frac{g_r}{2} \mid E_L \mid^2 E_P - \frac{g_r}{2} \mid E_S \mid^2 E_P \tag{1}$$

$$\frac{\partial E_L}{\partial z} + \frac{n}{c}\frac{\partial E_L}{\partial t} = \frac{g_r}{2} \mid E_P \mid^2 E_L + i\frac{\gamma_e \omega_L}{4\rho_0 nc} Q E_S \tag{2}$$

$$\frac{\partial E_S}{\partial z} - \frac{n}{c}\frac{\partial E_S}{\partial t} = 2i\gamma \mid E_P \mid^2 E_S + \frac{g_r}{2} \mid E_P \mid^2 E_S - i\frac{\gamma_e \omega_S}{4\rho_0 nc} Q^* E_L \tag{3}$$

$$\frac{\partial Q}{\partial t} + \frac{1}{2}\Gamma_B Q = i\frac{\gamma_e k_Q^2}{16\pi\Omega} E_L E_S^* \tag{4}$$

The Raman pump field E_P is backward-propagating (in the -z-direction). The single-frequency signal E_L that is amplified (i.e., the Raman Stokes field) is forward-propagating in the +z-direction. The signal acts as a pump for the SBS process, which, we repeat, is a severe limitation to signal power scaling. The Brillouin Stokes field E_S propagates in the -z-direction. Furthermore, ω_P, ω_L and ω_S are the angular frequencies of the Raman pump wave, signal wave and the Brillouin Stokes wave. All these waves are assumed to be slowly varying in time and space. The Raman interaction is included by the Raman gain coefficient g_r, whereas γ is the nonlinear coefficient related to the nonlinear refractive index n_2 [17] and n is the refractive index. As it comes to the Brillouin interaction, the acoustic phonon field Q is driven by the signal and Brillouin Stokes fields. It propagates in the +z direction with wavenumber k_Q and angular frequency $\Omega_B = \omega_L - \omega_S$. Furthermore, $\Gamma_B/2\pi$ is the intrinsic Brillouin gain bandwidth, γ_e is the electrostrictive coefficient, and ρ_0 is the average density of the material. These parameters correspond to a Brillouin gain coefficient $g_B = 7.28$ pm/W, which is lower than in a standard silica fiber but agrees with the value measured at 1550 nm [26] for a highly nonlinear fiber.

The Brillouin frequency shift ($\Omega_B/2\pi$) is 9.26 GHz ($\sim$0.1 nm) at 1651 nm (our signal wavelength). This is much smaller than the Raman gain bandwidth of several THz. Therefore, the Brillouin Stokes wave undergoes Raman amplification, too, and the Raman pump is depleted by both the signal and the Brillouin Stokes wave. Equation (1) describes the Raman pump evolution. The right-hand side (RHS) represents SRS from the pump to the signal and the Brillouin Stokes wave. Equation (2) describes the signal evolution, with amplification through SRS and depletion by SBS on the RHS. Equation (3) describes the Brillouin Stokes wave. The first term in the RHS of Eq. (3) shows the cross-phase modulation (XPM) of the Brillouin Stokes wave induced

by the intensity-modulated Raman pump. The following terms represent Raman and Brillouin gain. Equation (4) describes the acoustic wave, and how it is driven by the signal and Stokes waves. Because the speed of sound is low compared to light waves, its propagation is not included explicity in the equations for the SBS interaction.

Self-phase modulation (SPM) of the Raman pump is not included, either. The linewidth of the Raman pump is typically relatively large, and we do not expect the additional spectral broadening from SPM to be significant. We also exclude cross-modulation induced by the Raman pump on the signal since the two waves are counter-propagating. An important point is that the possible pump modulation formats may be limited by unwanted SRS in the direction of the pump wave. This SRS, which amplifies the Brillouin Stokes wave, can become unacceptably high. In the absence of dispersion, this is largely determined by the peak power of the Raman pump. The presence of dispersion leads to walk-off between the Raman pump and Brillouin Stokes wave and thus an averaging effect which reduces the effective pump peak power. However, although the fiber used experimentally has significant normal dispersion, it is not included in our model since it is not important with the relatively short fiber and parameters we used in the simulations. We also neglect parametric amplification of the Brillouin Stokes wave induced by the Raman pump. The lack of phase-matching justifies this in the normal dispersion regime. We also ignore the background propagation loss.

We use the above model to demonstrate SBS threshold enhancement by intensity-modulating the Raman pump. We numerically integrated the coupled-amplitude equations of Eq. (1)-(4) using the method of characteristics [24]. A Raman pump at 1542 nm is launched at the far (tail) end of the fiber, and a signal (Raman Stokes) at 1651 nm is launched at the head (input) end. We also launch a power of 1 μ W to seed the Brillouin Stokes wave in the tail end of the fiber. This is equivalent to the seeding through (primarily) thermally induced spontaneous Brillouin scattering that occurs throughout the fiber [27], [28]. For the fiber, we use the parameter values given in the Table I, which agree with those used experimentally.

We use a time step of 1 ns in the simulations, which allows us to capture the Brillouin dynamics. However, the high temporal resolution limits the fiber length we can simulate, due to prohibitive run times. We chose to use a fiber length of 40 m in the simulations, which is much shorter than the length used experimentally. We also aim for a relatively low Raman gain of up to $\sim$ 10 dB for the signal. This reduces the problem of unwanted Raman amplification of the Brillouin Stokes wave. Basic SRS equations then suggests that a pump power of around 20 W and an input signal power of 2 W allows for efficient Raman conversion in 40 m, in the absence of SBS. The presence of SBS in the simulations reduces the conversion efficiency, but we still obtained stable solutions with these parameters. The parameter space is quite large, and in addition to run-time, numerical convergence was problematic with some parameters.

Figure 2 shows baseline simulation results without modulation of the Raman pump. The signal output power becomes 4.6 W. This is limited by the growth of the Brillouin Stokes wave. This reaches 0.32 W of power which is 55 dB higher than the Brillouin Stokes seeding of 1-μ W. For comparison, simulations without any SBS led to a signal output power of 5.1 W, which was limited by the fiber length rather than by SBS.

TABLE I
VALUES OF PARAMETERS MEASURED FOR THE HIGHLY NONLINEAR FIBER USED IN THE EXPERIMENTS AND VALUES INPUT TO THE SIMULATIONS

Parameters	Measured/ Experimental value	Value in simulations
Attenuation coefficient (α dB)	0.65 dB/km	Not used (0 dB/km)
Brillouin gain coefficient (g_B)	7.28 pm/W†	Same
Raman gain coefficient (g_R)	33 fm/W	Same
Nonlinear coefficient (γ)	9.71 $km^{-1}W^{-1}$	Same
Dispersion parameter (D)	-20 ps/nm/km*	Not used (0 ps/nm/km)
Raman-pump-to-signal walk-off rate	2.16 ns/km*	Not used (0 ns/km)
Effective core area	9.4 μm^2	Same
Fiber length	5000 m	40 m
Brillouin frequency shift ($\Omega_B/2\pi$)	9.26 GHz†	Same
Brillouin gain bandwidth Half-width at half-maximum ($\Gamma_B/2\pi$)	32 MHz†	Same
Pump wavelength (λ_p)	1542 nm	Same
Signal wavelength (λ_s)	1651 nm	Same
Acoustic phonon lifetime	10 ns‡	Not used

†Measured at 1550 nm and recalculated to 1651 nm.
*From [30].
‡ Calculated from the Brillouin gain bandwidth.

We next consider an intensity-modulated Raman pump having the same average power of 20 W. We use a simple sinusoidal modulation with period 20 ns (frequency 50 MHz). The instantaneous Raman pump input power is shown in Fig. 3 a. Figure 3b and 3(c) show how the average power of the Raman pump, signal, and Brillouin Stokes evolve along the fiber. Fig. 3 d and 3(e) show the output Brillouin Stokes spectrum. Figure 3 f shows the output signal spectrum. The input signal power was adjusted to 2.18 W (as opposed to 2 W in Fig. 2b) in Fig. 3 to get the same output signal power as in Fig. 2b . The reduction in average-power gain may be due to the number of pump modulation cycles that the signal sees. This is relatively small, especially in the part of the fiber where the signal is strong. Whereas the evolutions of the Raman pump and signal are nearly identical with and without modulation, the Brillouin Stokes power is reduced significantly. The peak Brillouin spectral power density is 27 dB higher in Fig. 2 d than in Fig. 3 d. The signal interacts only with the Stokes power within the Brillouin gain bandwidth, and this is reduced by 34 dB in the Stokes output spectrum. The increase in total Stokes power from the 1 μW seed becomes 32 dB, so the Brillouin gain is reduced by 23 dB compared to the 55 dB in the unmodulated case.

III. EXPERIMENTAL SETUP

Our experimental setup is shown in Fig. 4. It is fully fiberized. For seeding of the signal, we used a DFB diode laser at

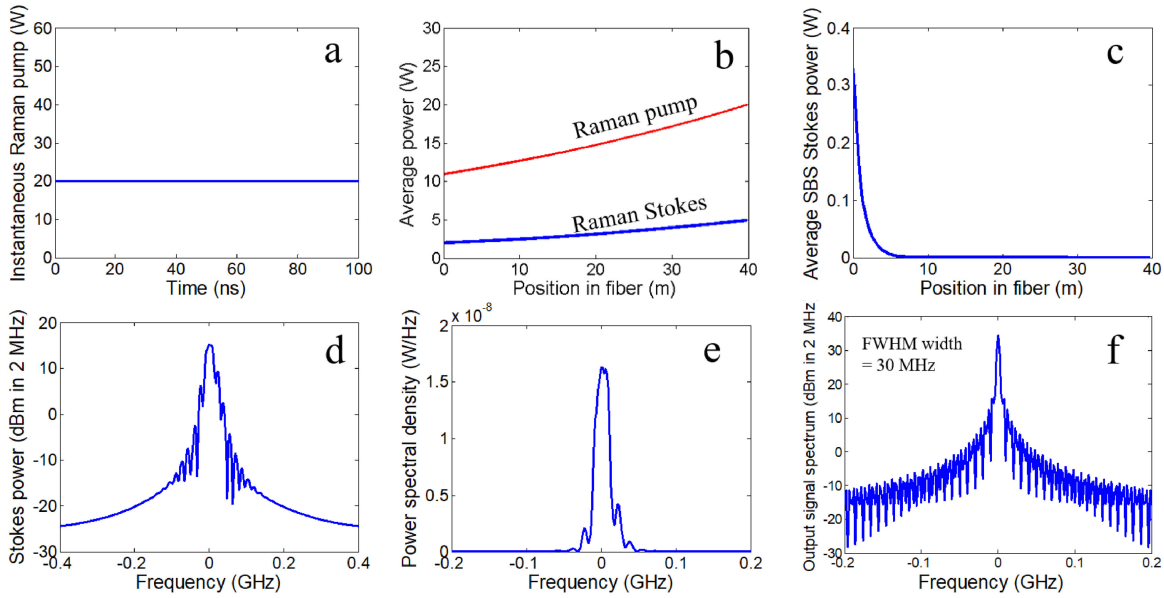

Fig. 2. Simulation results for 20 W continuous-wave pumping and 2 W of signal seeding. (a) Instantaneous Raman pump power, (b) time averaged Raman pump power and time averaged signal power (Raman Stokes) along the length of the fiber, (c) time averaged Brillouin Stokes power along the length of the fiber, (d) output optical spectrum of the Brillouin Stokes with resolution of 2 MHz with logarithmic and (e) linear units and (f) output signal optical spectrum with resolution of 2 MHz.

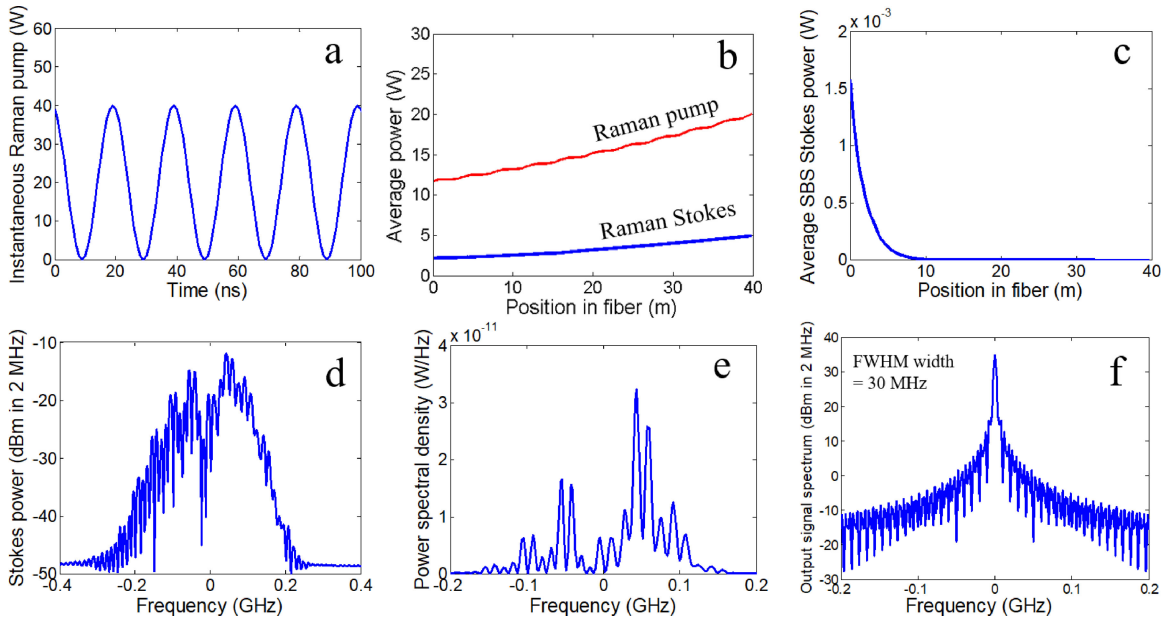

Fig. 3. Simulation results for sinusoidally modulated pumping with 20 W average power and 2.18 W of signal seeding. (a) Instantaneous Raman pump power, (b) time averaged Raman pump power and time averaged signal power (Raman Stokes) along the length of the fiber, (c) time averaged Brillouin Stokes power along the length of. the fiber, (d) output optical spectrum of the Brillouin Stokes with resolution of 2 MHz in logarithmic and (e) linear units and (f) output signal optical spectrum with resolution of 2 MHz.

wavelength of 1651 nm with 2 mW of fiber-coupled power at the output of an isolator. The manufacturer specifies the linewidth to be less than 1 MHz. The signal is then amplified in a Raman pre-amplifier with counter-propagating continuous-wave (CW) pumping. The output of the pre-amplifier is passed through another isolator into the main FRA, with launched signal power variable up to 30 mW. Both FRAs are pumped at a wavelength λ_p of 1542 nm. The main FRA is based on a 5-km long highly nonlinear fiber (HNLF) from Sumitomo with measured parameter values given in Table I. The dispersion is normal and nearly constant at -20 ps/nm/km between 1542 and 1651 nm. The walk-off between the co-propagating pump and Brillouin Stokes wave becomes 2.16 ns/km (measurements by Farrell [30]), and thus 10.8 ns in 5 km of fiber. The effective length becomes $[1 - e^{(-\alpha_{dB} L/4.343)}]4.343/\alpha_{\mathrm{dB}} = 3.52$ km. The separation between the Raman pump wavelength and the signal becomes

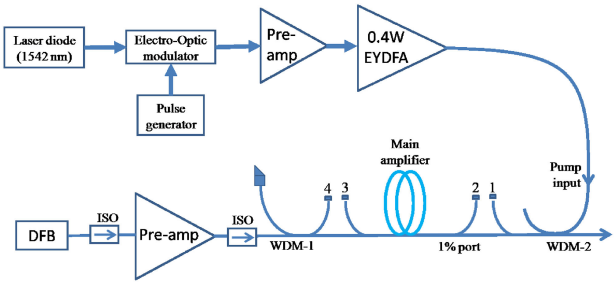

Fig. 4. Schematic diagram of the experimental set up to demonstrate SBS suppression in intensity modulated counter pumped Raman amplifier. EOM: electro-optic modulator, AOM: acousto-optic modulator, AWG: arbitrary waveform generator, EYDFA: erbium-ytterbium co-doped fiber amplifier, ISO: isolator.

13.1 THz or 428 cm^{-1}. This is marginally larger than the separation of 410 cm^{-1} to the Raman peak at 1646 nm in the HNLF.

Several 1% taps (ports 1, 2, 3 and 4) are used to monitor the forward and backward-propagating waves. An optical spectrum analyzer (OSA; Advantest Q8384) with smallest resolution bandwidth of 0.01 nm captures optical spectra. Unless otherwise stated, temporal traces of the different lightwaves are captured by a photodetector (Electro-Optics Technology ET-3500F, bandwidth $>$ 10 GHz) and an oscilloscope (Agilent Infiniium 54855A, bandwidth 6 GHz). The overall measurement bandwidth is estimated to 5.1 GHz. All fiber ends including those of the taps and WDMs are terminated with angled connectors (FC/APC) to suppress feedback.

The 1542-nm pump source is a fiber-master oscillator-power amplifier (MOPA) seeded by a 1542-nm Fabry-Perot diode laser. This is intensity-modulated by an electro-optic modulator (EOM), driven directly by a pulse generator with 3-GHz maximum PRF (Agilent 8133A) and set to generate rectangular pulses at $V_\pi = 3.3$ V. The shortest pulse duration that can be set in the pulse generator is 50 ps, but the actual duration of the electrical pulses may be limited to a larger value. According to specificationof the signal generator, the 10%-90% risetime is below 100 ps, and is typically below 60 ps. At a setting of 50 ps, we measured the pulse duration with the generator connected directly to a 20-GHz oscilloscope (Tektronix DSA 7200B) to 95 ps, but this is likely to be affected slightly by the oscilloscope bandwidth. We also measured the optical pulses at the output of the EOM with the 20-GHz oscilloscope. The actual optical pulses may become longer because of the finite bandwidth of the EOM, but may also become shorter and sharper because of the nonlinear response of the EOM. We were able to measure optical pulse durations as short as 100 ps, but we expect that the actual duration with 50 ps setting is shorter, since the overall behavior of the MOPA changed when we changed the set duration from 50 to 100 ps. In the text we generally use set pulse durations. Table II shows how these correspond to actual pulse durations.

The output from the EOM is boosted in an erbium-doped fiber amplifier followed by an Erbium:ytterbium co-doped fiber amplifier and then launched into the FRA as a pump with maximum average power of 0.4 W. Fused-fiber wavelength division multiplexers (WDMs) with center wavelengths of 1550 and 1650 nm are used to combine as well as separate the pump and signal, so that WDM-1 in Fig. 4 removes residual Raman pump power.

TABLE II
ACTUAL DURATION OF OPTICAL PULSE VS. GENERATOR SETTING

Set pulse duration	Actual duration of optical pulse
50 ps	60-100 ps
100 ps	90-120 ps
150 ps and above	set value $\pm$10 ps

IV. EXPERIMENTAL RESULTS

We first compare the performance of the FRA with CW and modulated pump. For all experimental results we report, the average (or CW) pump power P_p was at the highest available power of 0.4 W. At first, the modulated Raman pump comprises on-off-modulated approximately rectangular pulses at 400 MHz pulse repetition frequency (PRF). The pump pulse energy E_p becomes 1 nJ. The pulse period T of 2.5 ns is considerably smaller than the 10.8 ns of total walk-off between Raman pump and Brillouin Stokes in the fiber. The pulse duty cycle is varied between 10% and 90%, for pulse duration τ_p between 0.25 and 2.25 ns. At 0.4 W of pump power, the XPM phase shift induced by one pump pulse at 1 nJ of energy within the walk-off length L_{wo} is given by $\phi_{XPM} = (4/3)\gamma L_{wo} E_p/\tau_p = (4/3)\gamma\tau_p[D(\lambda_s - \lambda_p)]^{-1} P_p T/\tau_p = (4/3)\gamma[D(\lambda_s - \lambda_p)]^{-1} P_p T = 6$ rad, independently of the duty cycle. This disregards the variation of the pump power along the fiber, and within the walk-off length. The factor (4/3) applies for XPM between randomly polarized waves (so we no longer assume the waves to be linearly co-polarized). The phase shift then broadens the Brillouin Stokes wave and generates several spectral lines with 400-MHz separation. This is nearly an order-of-magnitude larger than the Brillouin linewidth measured in this fiber, so the power shifted to those lines will not stimulate any more Brillouin scattering (This is different from the simulations in Fig. 3, in which the pump modulation frequency is comparable to the Brillouin linewidth.) The highest signal output power is reached for 30% duty cycle. With larger duty cycle than 30%, the SBS suppression becomes weaker. Figure 5 a plots the output Stokes signal power against the input signal seed power for pumping with 0.4 W average power CW and modulated with 30% duty cycle. The small-signal gain becomes 12 dB for both modulated and CW pumping, for signal input powers up to 10 mW, in fair agreement with simple calculations without SBS. The pump modulation format captured through port 1 (at the pump input) is shown in Fig. 5b . As can be seen in Fig. 5 a, the maximum output signal power of 0.24 W with modulated pumping is improved by 4.7 dB, compared to CW pumping. It is reached for a signal input power of 25 mW, at which point the gain becomes 9.8 dB, again in fair agreement with simple simulations without SBS. Note however that different pump powers lead to different maximum signal powers, and to smaller as well as larger improvements. Pump PRFs in the range 0.3 GHz to 1 GHz gave comparable results. The single-pulse XPM phase shift in one walk-off length, neglecting pump depletion, becomes 8.0 rad (0.3 GHz) and 2.4 rad (1 GHz).

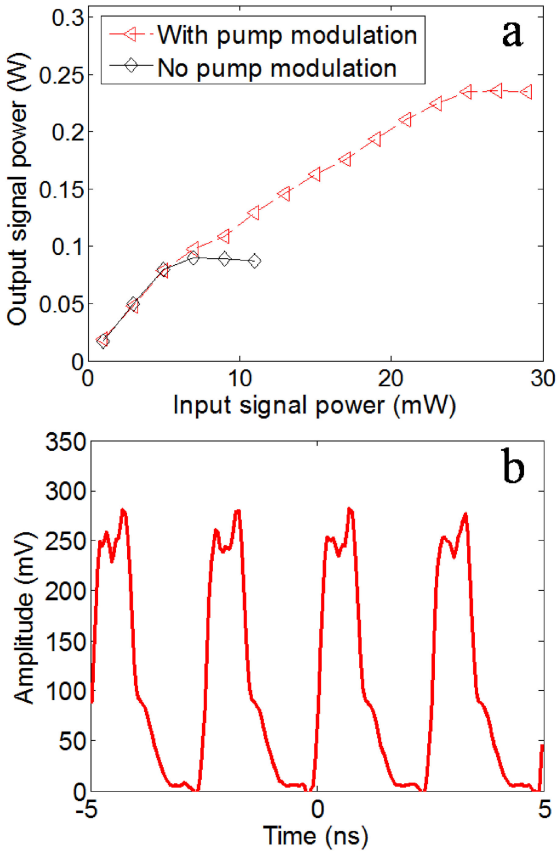

Fig. 5. (a) Output signal power with average Raman pump power of 0.4 W for CW pumping and pumping with pulses (PRF 400 MHz, duty cycle 30%), (b) temporal trace of Raman pump pulses.

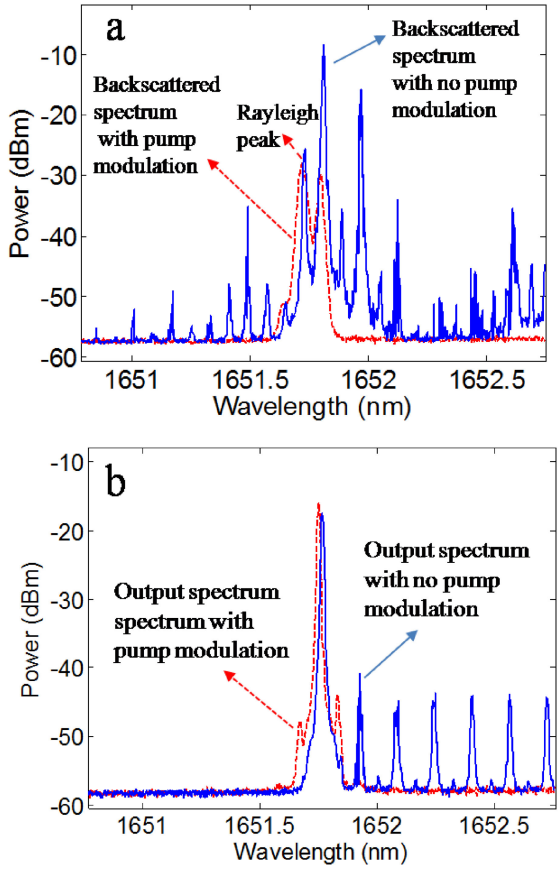

Fig. 6. Spectra for CW and pulsed Raman pumping for (a) backscattered light collected at port 3 (b) output signal collected at port 2. Average pump power 0.4 W, PRF 400 MHz, pump duty cycle 30 %, signal input power 12 mW. Resolution bandwidth 0.01 nm. The absolute vertical scaling is different in the two graphs.

Figure 6 shows forward and backward optical spectra at 12-mW of input seed power for CW and modulated pump (30% duty cycle). In the backward direction (Fig. 6 a), CW pumping leads to several Brillouin lines up to 17 dB higher than the Rayleigh-scattered signal line. These lines, which should not be confused with the much denser spectral lines within a single Brillouin Stokes order due to the periodic modulation, arise from (cascaded) SBS, which severely limits the output power. By contrast, the backscattered spectrum with modulated pump shows only the first Brillouin Stokes line, with peak ~2 dB lower than the Rayleigh peak. Also the forward output in Fig. 6b shows cascaded SBS lines with CW pumping, as back-scattered SBS-lines are again Brillouin-scattered (or Rayleigh-scattered) into the forward direction. The spectrum for the modulated Raman pump is distinctly improved with weak 1st-order Stokes and anti-Stokes components 30 dB below the signal peak and higher-order components essentially absent.

Next, we consider the effect of the pulse width at 1 GHz PRF, with 0.4 W average pump power. The single-pulse XPM phase shift within a walk-off length ϕ_{XPM} becomes 2.4 rad. The seed input power to the Raman amplifier is fixed to 20 mW, i.e., close to the highest available power. Figure 7 shows temporal traces for the input pump pulses at durations of 100 ps, 200 ps, 400 ps and 500 ps along with the corresponding backscattered optical spectra. The spectra show both the Brillouin and the Rayleigh peak. Figure 8 a plots the output signal power for 1 GHz PRF against the pump pulse duration. The maximum signal output power of 0.168 W is observed for 100 ps pulse duration, and the backscattered spectrum shows the Brillouin peak is lowest for this case. There is a slight reduction in the signal output power for 50 ps of set pulse duration. We tentatively attribute this to higher backward Raman amplification of the Brillouin Stokes wave, which depletes the Raman pump power. This is supported by the increase in total backward output power at 1.65 μ m (Fig. 8b) and decrease in the transmitted Raman pump power at 1550 nm (Fig. 8c) for 50 ps set duration. However, Fig. 8 d shows the spectral power of the 1^{st} Brillouin Stokes peak relative to that of the Rayleigh peak. According to this, the relative SBS peak is significantly higher for 50 ps pulse duration. This is surprising, but could perhaps be a result of details in the pulse shape or significant pump energy between pump pulses at this relatively low duty cycle (nominally 5%). Any such energy reduces the XPM for a given average power.

The lowest achievable output signal power of 0.138 W is observed for 500 ps pulse duration, and the spectrum shows the highest Brillouin peak with two cascaded Brillouin components appearing at longer wavelengths. We attribute this to a slow buildup of the XPM due to the low pump peak power. We also note that in many cases, and possibly even in all cases, higher

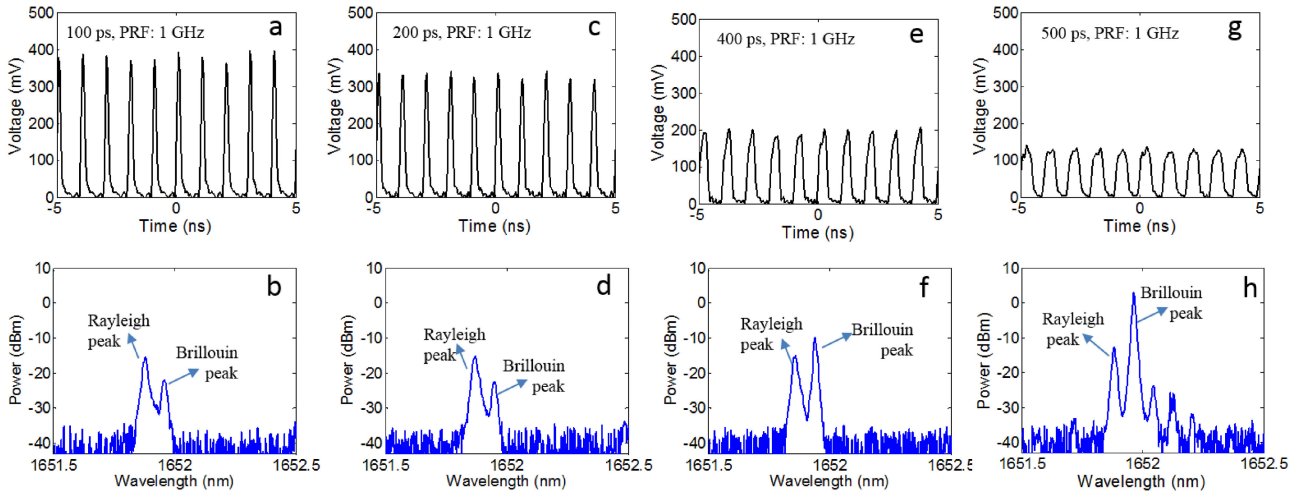

Fig. 7. Raman pump temporal formats with average power of 0.4 W for PRF of 1 GHz and pulse duration of (a) 100 ps, (c) 200 ps, (e) 400 ps, and (f) 500 ps. Corresponding optical spectra (uncalibrated) of the backscattered light is plotted in (b), (d), (f) and (h), respectively. Resolution bandwidth 0.01 nm.

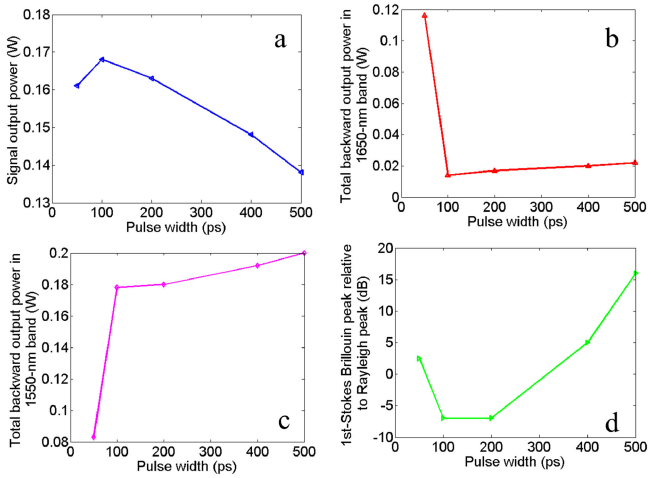

Fig. 8. Dependence on the set Raman pump pulse duration at 1-GHz PRF of the following quantities: (a) Signal output power, (b) total backward output power in the 1650-nm band, (c) total backward output power in the 1550-nm band and (d) peak spectral power of the 1st Brillouin Stokes peak relative to the Rayleigh peak.

pump power than we had available would allow for higher signal output power. We expect this would increase the difference in signal output power for different pulse durations.

We also investigated the effect of the PRF on the SBS suppression, for a fixed set pulse duration of 50 ps. Again, the average Raman pump power was 0.4 W and the signal seed power was 20 mW. Similarly to before, Fig. 9 shows temporal traces of the input pump pulses along with optical spectra of the backscattered light. Note however that the absolute vertical scaling of the spectra is different in Fig. 7 and Fig. 9. Figure 10 a plots the output signal power for the different modulation frequencies. The maximum output signal power of 0.178 W is observed for 1.5 GHz PRF, for which the nominal nonlinear phase shift induced by a single pump pulse (neglecting Raman pump depletion), ϕ_{XPM}, becomes 1.6 rad. A modulation frequency of 3 GHz leads to the lowest output signal power of 0.13 W. Here the pump pulse energy is so low that the SBS is limiting the power scaling as ϕ_{XPM} is only 0.8 rad. See also Fig. 9 h, which shows the buildup of the Brillouin peak for 3 GHz PRF. For lower PRF than 1.5 GHz there is a small drop in power at 1 GHz, and then it drops more significantly at 0.2 GHz. Again, this may be due to higher backward Raman amplification of the Brillouin Stokes wave, which depletes the Raman pump power. This is consistent with the backward spectrum of Fig. 9b for 0.2 GHz, which has much higher power (120 mW) than the other spectra in Fig. 9 (10–20 mW). Figure 10b and 10(c) plots the total backward power at wavelengths around 1.65 μ m (Raman Stokes range) and at around 1.55 μ m (Raman pump range), respectively, and Fig. 10d plots the power of the backscattered 1^{st} Brillouin Stokes spectral peak relative to the Rayleigh spectral peak. The Brillouin power generally decreases for lower PRF. Figure 10bconfirms the increase in backscattered 1.65-μ m power, and Fig. 10c in Raman pump depletion, for lower PRF.

V. Dicussion

The system is quite complex, and we have not found any definite design rules or criteria to attain a certain level of performance. Nevertheless, our results can still provide some understanding.

Our modulation is temporally periodic. Therefore, it imposes a periodic modulation of all affected spectra, which may be visible when the unmodulated linewidth is smaller than the modulation frequency. This was not the case for the XPM-broadening of the Brillouin Stokes spectrum in the simulations but is the case in the experiments (although the resolution of our optical spectra is too low to show this). The generated sidebands will then be outside the Brillouin gain bandwidth so only the central component of the Brillouin Stokes wave takes part in the SBS interaction. In the amplitude domain, this component is given by the average amplitude of the complex modal amplitude E (t), i.e $\int_0^T E_S(t)dt/T$. If we assume the lightwave is purely phase-modulated in a rectangular fashion (comprising two parts with

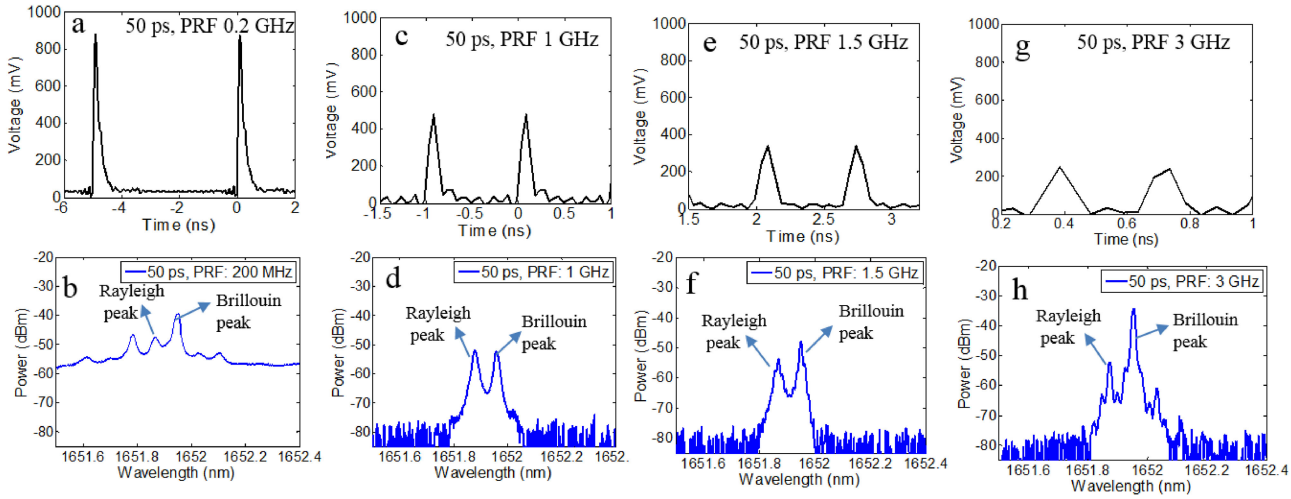

Fig. 9. Raman pump modulation formats with average power of 0.4 W captured in the oscilloscope for pulse duration of 50 ps and PRF of (a) 0.2 GHz, (c) 1 GHz, (e) 1.5 GHz, and (f) 3 GHz. Corresponding optical spectra of the backscattered light is plotted in (b), (d), (f) and (h), respectively. Resolution bandwidth 0.01 nm.

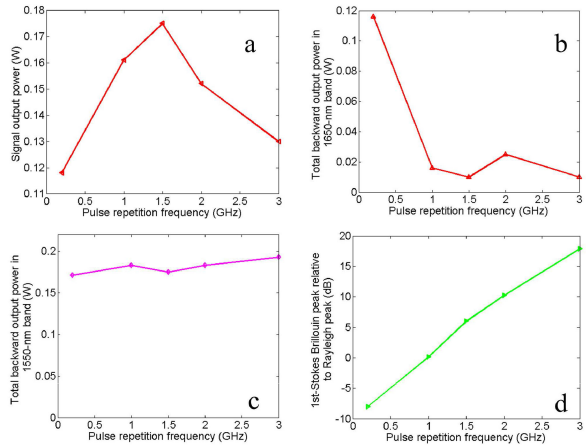

Fig. 10. (a) Dependence on the Raman pump pulse repetition frequency at 50-ps set pulse duration of the following quantities: (a) Signal output power, (b) total backward output power in the 1650-nm band, (c) total backward output power in the 1550-nm band and (d) peak spectral power of the 1st Brillouin Stokes peak relative to the Rayleigh peak.

different phase), then the average amplitude can be found by the addition of two phasors. For the average value to be substantially different from the unmodulated case, the phase difference between the two parts should be close to π radians. If the phase difference equals π rad and the two parts are equal in amplitude and duration (50% duty cycle), then the averaged amplitude is zero, and the Stokes wave does not stimulate any Brillouin scattering.

In this simplified case, a larger phase shift closer to 2π is worse than a phase shift of π. If the Raman pump and the Brillouin Stokes propagate with the same group velocity, then the XPM phase would build up along the whole fiber and may well reach 2π rad. If the phase difference is evenly distributed between 0 and 2π rad along the fiber then it is easy to show that the effective Stokes power is reduced by half, in case of 50% duty cycle .

In our experiments, however, the walk-off is significant. At 1 GHz PRF, the signal walks-off from the pump by one period of 1 ns in 464 m. From before, the phase shift induced by the pump on the Stokes wave as they walk through each other, and thus for one period, becomes $\phi_{XPM} = (4/3)\gamma L_{wo} E_p/\tau_p = (4/3)\gamma\tau_p[D(\lambda_s - \lambda_p)]^{-1} P_p T/\tau_p = (4/3)\gamma[D(\lambda_s - \lambda_p)]^{-1} P_p T = 2.4$ rad. This is less than π rad, but still large enough for the two phasors to cancel each other to a significant degree. Note here that this is the amplitude, so if the resulting phasor is reduced by, e.g., 50% then the power in the fundamental Stokes component which stimulates the Brillouin scattering, is reduced by 75%.

Because of the walk-off, the phase modulation of the Brillouin Stokes wave will not build up in a rectangular-like manner. The resulting more complicated build-up may mean that the optimum peak value of ϕ_{XPM} is greater than π rad, and may be much greater. However, we would still expect that a value smaller than π rad is less effective. Although Fig. 10 a shows a maximum output power for 1.5 GHz PRF for which we calculate ϕ_{XPM} to only 1.6 rad, the Brillouin level is lower at 1 GHz ($\phi_{XPM} = 2.4$ rad), and the lower signal output power for 1 GHz may depend on other factors. For example, even though the residual Raman pump power is similar for all PRFs in Fig. 10c, the induced Raman gain also depends on how the Raman pump power evolves along the fiber, and that may be more favorable for 1.5 GHz. We also note that with higher pump power, 1 GHz PRF may allow for higher signal output power than 1.5 GHz.

Although the duty cycle of the pump pulse duration matters, it does not influence the phase shift ϕ_{XPM} per pulse at fixed PRF and average pump power (if pump depletion can be neglected.) If the pump duty cycle is, say, 10% (100 ps @ 1 GHz) then the pump shifts relative to the Brillouin Stokes by 100 ps in 46.4 m, and in the process induces a (peak) phase shift of 2.4 rad. This phase shift is gradually reached for an increasing fraction of the signal, until it is finally reached for the whole signal (if we neglect the depletion of the pump power), when the walk-off reaches 1 ns. In the process, the power in the fundamental Stokes component reaches a minimum when the pump signal walk-off is half of the period, if the Raman pump and Brillouin

Stokes powers are constant during this process. However, except for the very shortest pulses with 50 ps of set duration, the experimental results in Fig. 7 and 8 show higher signal output power and lower levels of SBS for shorter pulses. We tentatively attribute this to SRS and/or SBS within a walk-off length, which we did not consider in the simple phasor addition description. As it comes to SRS, the pump power that leads to 1 rad of XPM leads to approximately 1.53 dB of Raman gain. For the high pump pulse energies at 0.2 GHz PRF, the resulting Raman gain in one walk-off length becomes $\sim$ 18.3 dB, which we expect significantly modifies (and complicates) the interaction. In addition to an increase in the Raman pump depletion, the resulting modulation of the Brillouin Stokes wave also leads to spectral broadening through SPM. On the other hand, at 1 GHz PRF as used in Fig. 7 and 8, the Raman gain is only $\sim$ 3.66 dB. Given also the averaging that is a consequence of the walk-off and the periodic modulation, the increase in Raman pump depletion and SPM is then reduced and may be negligible.

The Brillouin gain, on the other hand, is considerably higher than the Raman gain. At a signal power of 0.15 W, it becomes 234 dB over the 464 m that corresponds to 1 ns of walk-off. Such high gains are unattainable and would deplete the signal in a fraction of the walk-off length. This implies it is necessary to suppress SBS already within the walk-off length corresponding to one modulation period, and averaging over the modulation and walk-off length may be questionable. According to the phasor addition picture, for best cancelation and SBS suppression it is good if the phase difference between phasors reaches a phase of π as quickly as possible, even if only with a relatively small fraction of the overall amplitude. Then, ideally at π phase difference, the relative amplitude of the weaker phasor will gradually increase, as the walk-off causes a larger fraction of the 1-ns period to be modulated. The rapid buildup of the nonlinear phase and the gradual increase of the phasor amplitude will happen with short pulses of high peak power. For example, with 100 ps duration and 1 GHz PRF, 2.4 rad of XPM is reached in 46.4 m, over which the Brillouin gain is a much more manageable 23.4 dB (approximately). The modulation then needs to suppress this, so it does not reach unsustainable levels as the Stokes wave propagates further down the fiber. Note also that the Raman amplification concomitant with the XPM can improve the cancellation of the phasors, insofar as it increases the amplitude of the phase-shifted phasor of the Brillouin Stokes wave, which is otherwise small due to the small duty cycle.

Our discussion has neglected pump depletion. The most obvious effect is that there is less XPM in the signal input end of the fiber, where the pump is weaker. On the other hand, also the signal is weak, which reduces the Brillouin gain and thus the rate of power transfer from the signal into the fundamental line of the Brillouin Stokes in the signal input end. This makes it easier for the XPM to induce the required phase modulation, though dispersion is also a factor in this.

The pump launch end may be more important. There, the rate of depletion can be high if the signal power is high. This will be a factor if the depletion is significant within the pump-signal walk-off distance (say, for PRF below 0.4 GHz in case of 0.4 W of average pump power).

The simulations and experiments combined show that the SBS threshold enhancement technique works for a wide range of parameters. The guidelines for selecting the pump modulation parameters for effective suppression are also given here. Foremost, the pump modulation frequency should be higher compared to the spontaneous Brillouin bandwidth if a periodic modulation is employed. Since the typical value of SBS bandwidth in fiber is 35 MHz, the pump modulation frequency should be higher than 35 MHz. However, our experimental results show that higher modulation frequencies in the range 1 GHz give better suppression. The peak power of the pump intensity modulation has to be such that it does not deplete the Raman pump power in the direction of the pump. The length of the fiber amplifier also plays an important role in the selection of the pump modulation parameters. Long dispersive fibers can see lower peak powers due to walk-off between the pump and signal. However, shorter fibers have less influence of the walk-off.

Finally, and importantly, we note that a broadening of the fiber's intrinsic Brillouin gain or the signal linewidth does not change the way the proposed suppression works, as long as the broadening is smaller than the modulation frequency so that the resulting Stokes spectrum still comprises distinct components. Such broadening is frequently used to reduce the Brillouin gain [7], [15], [29]. Thus, the proposed suppression combines well with established SBS suppression techniques. According to our simulations, our approach suppresses SBS also when the components are not distinct. However, the details become more difficult to analyze.

VI. Conclusion

In summary, we have presented and assessed pulsed backward-propagating pumping as a method for suppressing stimulated Brillouin scattering in fiber Raman amplifiers. This method is new to the best of our knowledge, and we expect it combines well with other SBS suppression approaches. The Raman pump induces cross-phase-modulation, which broadens the SBS Stokes wave beyond the intrinsic Brillouin bandwidth. The PRF of the Raman pump, the pulse duration, and fiber dispersion influences the achievable SBS suppression. We used a time-domain finite difference solver to demonstrate SBS suppression in a FRA with modulation frequency smaller than the SBS linewidth and with modest fiber length to reduce computer runtime. Experimentally, we demonstrated SBS suppression at PRF higher than the SBS linewidth in a 5-km long fiber with significant dispersion. We varied the PRF and the pump pulse duration, and concluded that the amount of SBS is determined by two processes. At low pump duty cycles, the high instantaneous pump power leads to undesired SRS backward-propagating together with the pump. At high pump duty-cycle, or at high PRF, the instantaneous pump power is too low and the resulting XPM thus insufficient for suppressing the SBS. The process and the importance of different parameters values are difficult to analyze, but we argue it is important that a pump pulse can induce a phase shift of at least approximately π rad on the Brillouin Stokes wave. Experimentally, we triple the SBS-limited output power

(4.7 dB increase) and reach a pump-to-signal power conversion efficiency of over 50%. We believe that the improvement can be even larger with further optimization and in systems with different parameters.

ACKNOWLEDGMENT

The authors would like to thank Sumitomo Electric Industries, Ltd. (Masashi Onishi, Masaaki Hirano and Takashi Sasaki) for providing the highly nonlinear fiber used in their experiments. The data for this work are accessible through the University of Southampton Institutional Research Repository (https://doi.org/10.5258/SOTON/D0777).

REFERENCES

[1] A. Liem, J. Limpert, H. Zellmer, and A. Tünnermann, "100-W single-frequency master-oscillator fiber power amplifier," *Opt. Lett.*, vol. 28, no. 17, pp. 1537–1539, Sep. 2003.

[2] Y. Jeong *et al.*, "Single-frequency, single-mode, plane-polarized ytterbium-doped fiber master oscillator power amplifier source with 264 W of output power," *Opt. Lett.*, vol. 30, no. 5, pp. 459–461, 2005.

[3] I. Dajani, C. Vergien, C. Robin, and B. Ward, "Investigations of single-frequency Raman fiber amplifiers operating at 1178 nm," *Opt. Express*, vol. 21, no. 10, pp. 12038–52, 2013.

[4] L. R. Taylor, Y. Feng, and D. B. Calia, "50 W CW visible laser source at 589 nm obtained via frequency doubling of three coherently combined narrow-band Raman fibre amplifiers," *Opt. Express*, vol. 18, no. 8, pp. 8540–8555, 2010.

[5] Y. Feng, L. Taylor, and D. B. Calia, "Multiwatts narrow linewidth fiber Raman amplifiers," *Opt. Express*, vol. 16, no. 15, pp. 10927–10932, 2008.

[6] A. Liu, "Suppressing stimulated Brillouin scattering in fiber amplifiers using nonuniform fiber and temperature gradient," *Opt. Express*, vol. 15, no. 3, pp. 977–984, 2007.

[7] N. Yoshizawa and T. Imai, "Stimulated Brillouin scattering suppression by means of applying strain distribution to fiber with cabling," *J. Lightw. Technol.*, vol. 11, no. 10, pp. 1518–1522, Oct. 1993.

[8] V. I. Kovalev and R. G. Harrison, "Suppression of stimulated Brillouin scattering in high-power single-frequency fiber amplifiers," *Opt. Lett.*, vol. 31, no. 2, pp. 161–163, 2006.

[9] S. Yoo, C. A. Codemard, Y. Jeong, J. K. Sahu, and J. Nilsson, "Analysis and optimization of acoustic speed profiles with large transverse variations for mitigation of stimulated Brillouin scattering in optical fibers," *Appl. Opt.*, vol. 49, no. 8, pp. 1388–99, Mar. 2010.

[10] P. D. Dragic, C. H. Liu, G. C. Papen, and A. Galvanauskas, "Optical fiber with an acoustic guiding layer for stimulated Brillouin scattering suppression," in *Proc. Conf. Lasers Electro-Opt./Quantum Electron. Laser Sci. Photon. Appl., Syst. Technol.*, 2005, Paper CThZ3.

[11] M. Li *et al.*, "Al/Ge co-doped large mode area fiber with high SBS threshold," *Opt. Express*, vol. 15, pp. 8290–8299, 2007.

[12] M. D. Mermelstein *et al.*, "11.2 dB SBS gain suppression in a large mode area Yb-doped optical fiber," *Proc. SPIE*, vol. 6873, pp. U63–U69, 2008.

[13] K. Shiraki, M. Ohashi, and M. Tateda, "Suppression of stimulated Brillouin scattering in a fibre by changing the core radius," *Electron. Lett.*, vol. 31, no. 8. pp. 668–669, 1995.

[14] J. A. Nagel *et al.*, "High-power narrow-linewidth continuous-wave Raman amplifier at 1270 nm," *IEEE Photon. Technol. Lett.*, vol. 23, no. 9, pp. 585–587, May 2011.

[15] C. Zeringue, I. Dajani, S. Naderi, G. T. Moore, and C. Robin, "A theoretical study of transient stimulated Brillouin scattering in optical fibers seeded with phase-modulated light," *Opt. Express*, vol. 20, no. 19, pp. 21196–213, Sep. 2012.

[16] A. V. Harish and J. Nilsson, "Optimization of phase modulation with arbitrary waveform generators for optical spectral control and suppression of stimulated Brillouin scattering," *Opt. Express*, vol. 23, no. 6, pp. 6988–6999, 2015.

[17] H. Lee, Y. Hana, J. Kima, W. Yanga, S. K. Limb, and C. An, "Effect of external phase modulation on suppression of stimulated Brillouin scattering in an optical transmission system using fibre lasers," *Proc. SPIE*, vol. 4579, pp. 350–354, 2001.

[18] S. S. Lee, H. J. Lee, W. Seo, and S. G. Lee, "Stimulated Brillouin scattering suppression using cross-phase modulation induced by an optical supervisory channel in WDM links," *IEEE Photon. Technol. Lett.*, vol. 13, no. 7, pp. 741–743, Jul. 2001.

[19] F. H. Tithi and M. S. Islam, "Suppression of stimulated Brillouin scattering effect using nonlinear phase modulation," in *Proc. Int. Conf. Elect. Comput. Eng.*, Dec. 2010, pp. 135–138.

[20] Y. Horiuchi, S. Yamamoto, and S. Akiba, "Stimulated Brillouin scattering suppression effects induced by cross-phase modulation in high power WDM repeaterless transmission," *Electron. Lett.*, vol. 34, no. 4, pp. 390–391, 1998.

[21] G. Ravet, A. F. Fotiadi, M. Blondel, and P. Megret, "Suppression of stimulated Brillouin scattering with a Raman fiber amplifier," in *Proc. IEEE Lasers Electro-Opt. Soc.*, Ghent, Belgium, 2004, pp. 199–204.

[22] S. Gray, M. Vasilyev, and K. Jepsen, "Spectral broadening of double Rayleigh backscattering in a distributed Raman amplifier," in *Opt. Fiber Commun. Conf. Exhib. Tech. Dig. Postconf. Ed.*, 2001, Paper MA2.

[23] M. Vasilyev, S. Gray, and V. M. Ricci, "Pump intensity noise and ASE spectrum of Raman amplification in non-zero dispersion-shifted fibers," in *Proc. Opt. Amplifiers Appl.*, 2001, Paper OMC3.

[24] M. C. P. Huy *et al.*, "Lowering backward Raman and Brillouin scattering in waveguide Raman wavelength converters," *J. Eur. Opt. Soc.*, vol. 13, no. 31, 2017. [Online]. Available: https://jeos.springeropen.com/articles/10.1186/s41476-017-0059-3

[25] R. W. Boyd, K. Rzaewski, and P. Narum, "Noise initiation of stimulated Brillouin scattering," *Phys. Rev. A*, vol. 42, no. 9, pp. 5514–5521, 1990.

[26] M. Nikles, L. Thévenaz, and P. A. Robert, "Brillouin gain spectrum characterization in single-mode optical fibers," *J. Lightw. Technol.*, vol. 15, no. 10, pp. 1842–1851, Oct. 1997.

[27] A. Liu, X. Chen, M.-J. Li, J. Wang, D. T. Walton, and L. A. Zenteno, "Comprehensive modeling of single frequency fiber amplifiers for mitigating stimulated Brillouin scattering," *J. Lightw. Technol.*, vol. 27, no. 13, pp. 2189–2198, Jul. 2009.

[28] A. Liu, X. Chen, M.-J. Li, J. Wang, D. T. Walton, and L. A. Zenteno, "Suppressing nonlinear effects for power scaling of high power fiber lasers," *Proc. SPIE*, vol. 6781, Nov. 2007, Art. no. 67810H.

[29] A. V Harish and J. Nilsson, "Optimization of phase modulation formats for suppression of stimulated Brillouin scattering in optical fibers," *IEEE J. Sel. Top. Quantum Electron.*, vol. 24, no. 3, pp. 1–10, May/Jun. 2018.

[30] C. Farrell, "Pulse-pumping of cascaded Raman fibre amplifiers," Ph.D. dissertation, Fac. Eng., Sci. Math. Optoelectron. Res. Centre, Univ. Southampton, Southampton, U.K., 2010.

Achar Vasant Harish received the Master of Science degree from the Indian Institute of Technology Madras (IIT-M), Chennai, India, and the Ph.D. degree from the Optoelectronics Research Centre (ORC), University of Southampton, Southampton, U.K., in 2017. He has worked on optical fiber amplifiers and non-linear fiber optics at ORC and non-destructive testing with optical fiber sensors at IIT-M. He has published more than 20 scientific articles. His current research interests include suppression of stimulated Brillouin scattering in high-power optical fiber amplifiers, nonlinear optics, optofluidics, mitigation of thermal mode instability in fiber lasers, advanced optical modulation, and non-destructive testing of structures using fiber Bragg gratings.

Johan Nilsson received the Ph.D. degree in engineering science from the Royal Institute of Technology, Stockholm, Sweden, in 1994, for research on optical amplification. Since then, he has worked on optical amplifiers and amplification in lightwave systems, optical communications, and guided-wave lasers, first at Samsung Electronics and later at Optoelectronics Research Centre (ORC), University of Southampton. He is currently a Professor with the ORC, University of Southampton, and the head of the High Power Fiber Lasers research group. He has published more than 400 scientific articles. His research has covered system, fabrication, and materials aspects, and, in particular, device aspects of high-power fiber lasers and erbium-doped fiber amplifiers. He is a Fellow of the OSA and the SPIE, and a consultant to, and co-founder of, SPI Lasers. He is a member of the advisory board of the *Journal of the Optical Society of Korea* and was a Guest Editor of two issues on high-power fiber lasers in the IEEE JOURNAL OF SELECTED TOPICS IN QUANTUM ELECTRONICS in 2009. He is the former Chair of the Laser Science and Engineering technical group in OSA's Science and Engineering Council and currently the Program Chair for Advanced Solid State Lasers Conference.